Secretome analysis of rat osteoblasts during icariin treatment induced osteogenesis

WEIQING QIAN[1*], YAN SU[2*], YAJIE ZHANG[3], NIANWEI YAO[1], NIN GU[4], XU ZHANG[5] and HONG YIN[1]

[1]Department of Orthopedics, The 3rd Affiliated Hospital of Nanjing University of Chinese Medicine, Nanjing, Jiangsu 210001; [2]Reproductive Center, Obstetrics and Gynecology Hospital Affiliated to Nanjing Medical University; [3]Laboratory Center; [4]Cardiovascular Department, The 3rd Affiliated Hospital of Nanjing University of Chinese Medicine; [5]School of Medicine and Life Sciences, Nanjing University of Chinese Medicine, Nanjing, Jiangsu 210023, P.R. China

Received September 15, 2017; Accepted January 15, 2018

DOI: 10.3892/mmr.2018.8715

Abstract. Osteoporosis is a serious public health problem and icariin (ICA) is the active component of the *Epimedium sagittatum*, a traditional Chinese medicinal herb. The present study aimed to investigate the effects and underlying mechanisms of ICA as a potential therapy for osteoporosis. Calvaria osteoblasts were isolated from newborn rats and treated with ICA. Cell viability, apoptosis, alkaline phosphatase activity and calcium deposition were analyzed. Bioinformatics analyses were performed to identify differentially expressed proteins (DEPs) in response to ICA treatment. Western blot analysis was performed to validate the expression of DEPs. ICA administration promoted osteoblast viability, alkaline phosphatase activity, calcium deposition and inhibited osteoblast apoptosis. Secretome analysis of ICA-treated cells was performed using two-dimensional gel electrophoresis and matrix-assisted laser desorption/ionization time-of-flight mass spectrometry. A total of 56 DEPs were identified, including serpin family F member 1 (PEDF), protein disulfide isomerase family A, member 3 (PDIA3), nuclear protein, co-activator of histone transcription (NPAT), c-Myc and heat shock protein 70 (HSP70). These proteins were associated with signaling pathways, including Fas and p53. Bioinformatics and western blot analyses confirmed that the expression levels of the six DEPs were upregulated following ICA treatment. These genes may be directly or indirectly involved in ICA-mediated osteogenic differentiation and osteogenesis. It was demonstrated that ICA treatment promoted osteogenesis by modulating the expression of PEDF, PDIA3, NPAT and HSP70 through signaling pathways, including Fas and p53.

Correspondence to: Dr Hong Yin, Department of Orthopedics, The 3rd Affiliated Hospital of Nanjing University of Chinese Medicine, 1 Jinling Road, Nanjing, Jiangsu 210001, P.R. China
E-mail: hongyin0114@126.com

Dr Xu Zhang, School of Medicine and Life Sciences, Nanjing University of Chinese Medicine, 138 Xianlin Avenue, Nanjing, Jiangsu 210023, P.R. China
E-mail: zhangxu0114@126.com

*Contributed equally

Key words: icariin, osteoblasts, secretome, two-dimensional electrophoresis, western blot

Introduction

Osteoporosis, or porous bone, is a serious condition that impacts the health of hundreds of millions of people. In 2010, >158 million people suffered from osteoporotic fractures worldwide (1). Osteoporosis is typically prevalent in older populations, but can also occur in children and teenagers. Osteoporosis is characterized by a loss of bone mass or a reduction in bone mineral density (BMD) (2). Due to the complexity and number of causes of osteoporosis; however, the prevention and treatment of osteoporosis is a challenging process and existing therapies have a limited efficiency.

Estrogen deficiency (3), gene polymorphisms (4), menopause (5) and environmental factors, including smoking (6) may contribute to osteoporosis pathogenesis. Postmenopausal osteoporosis or reduction of BMD is partially due to estrogen deficiency (7). Previous studies focusing on osteoporosis drugs have demonstrated the risk factors or side-effects involved in osteoporosis treatment, such as increasing the risk of bone neoplasms, breast cancer and embolisms (8,9). Novel drugs with fewer adverse side effects are required for effective osteoporosis management.

Icariin (ICA) is a flavonol glycoside isolated from a traditional Chinese medicinal herb *Epimedium sagittatum*, the *Epimedium* genus (10). Previous studies focusing on the molecular mechanisms of ICA have demonstrated its anti-osteoporotic and osteogenic differentiation effects (11,12), as well as its involvement in estrogen biosynthesis, *in vivo* and *in vitro* (13,14). It is of note that ICA may regulate the expression of osteoporosis-associated factors, including the Wnt/β-catenin pathway, peroxisome proliferator-activated receptor γ (PPARγ), and bone morphogenetic protein (BMP) (15-17). Chen *et al* (15) demonstrated that the administration of ICA to an ovariectomized rat model of osteoporosis increases the expression of β-catenin pathway-associated proteins, including runt related transcription factor 2 and

low-density lipoprotein receptor related protein 6. Proteomics, transcriptomics, and metabolomics analyses have identified the dysregulation of mRNAs, proteins and metabolites associated with osteoporosis. However, there are limited studies that focus on the proteomics associated with the protective activity of ICA against osteoporosis, particularly the underlying mechanisms of ICA activity (18).

To further investigate the mechanisms of ICA against osteoporosis, the proteomics of ICA-treated calvaria osteoblasts were analyzed using matrix-assisted laser desorption/ionization time-of-flight mass spectrometry (MALDI-TOF-MS) analysis. Differentially expressed proteins (DEPs) in ICA-treated osteoblasts were identified and further investigated. The present study aimed to provide more information on the protective mechanisms of ICA against osteoporosis.

Materials and methods

Animals. All animal experimental protocols were approved by the Animal Care Committee of Nanjing University of Chinese Medicine (Nanjing, China) and were performed in accordance with the Guide for Care and Use of Laboratory Animals. A total of 10 Sprague-Dawley male rats (weighing 8-10 g), were obtained from Experimental Animal Center of Nanjing University of Chinese Medicine (Nanjing, China) within 24 h post-birth and kept in an incubator under 12-h light/dark cycle with a humidity of 45-75% at 19-27˚C, with free access to food and water.

Osteoblast isolation and cell culture procedure. The calvaria was dissected from surface-sterilized rats and subsequently soaked in 75% ethanol for 5-10 min at 4˚C. Isolation of calvaria osteoblasts was performed as previously described (19,20). Briefly, the frontal and parietal bone was separated, cut into fragments (1 mm^3), digested in 0.25% trypsin (Gibco; Thermo Fisher Scientific, Inc., Waltham, MA, USA) at 37˚C for 15 min and the precipitates following centrifugation at 750 x g and 4˚C for 5 min were treated with collagenase II (Sigma-Aldrich; Merck KGaA, Darmstadt, Germany) for 5 min for further digestion (19). Precipitated cells were subsequently suspended in Dulbecco's modified Eagle's medium (DMEM; Gibco; Thermo Fisher Scientific, Inc.) supplemented with 15% fetal bovine serum (FBS; Gibco; Thermo Fisher Scientific, Inc.) at 37˚C in 5% CO_2 for 24 h. Cells were then transferred to DMEM with 20% FBS. Medium was replaced every 2 days. For ICA (95.4%; cat. no I1286; Sigma-Aldrich; Merck KGaA) treatment, ICA was added into the cell cultures prior to incubation at concentration of 0, 10, and 20 μg/l at 37˚C in 5% CO_2 for 24 h. Each experiment was performed in triplicate.

Cell viability analysis. An MTT (Sigma-Aldrich; Merck KGaA) assay was performed to detect cell viability as previously described (16). Osteoblasts (50 cells/well) were seeded into 96-well plates and maintained in DMEM supplemented with 20% FBS (Gibco; Thermo Fisher Scientific) at 37˚C in 5% CO_2 for 24 h prior to treatment with 10 μg/l and 20 μg/l ICA for 5 days. The supernatant of cell cultures was subsequently discarded and 20 μl MTT solution (5 mg/ml) was added into each well and cells were incubated for a further 4 h. 150 μl DMSO was added and the optical density at an absorbance of 490 nm was determined using a microplate reader (Molecular Devices, LLC, Sunnyvale, CA, USA).

Cell cycle assay. Osteoblasts ($5x10^4$ cells/ml) were seeded into 6-well culture plates until 90% confluence. Cells were then treated with ICA for 48 h and harvested, fixed with 4% paraformaldehyde at 4˚C for 4 h, and stained with propidium iodide (PI) for 30 min in the dark at room temperature. For cell cycle analysis, the at G0/G1, S and G2/M phase distribution of 10,000 cells was determined using the BD FACS Calibur™ flow cytometer equipped with CellQuest Pro 5.1 software (BD Biosciences, San Jose, CA, USA). Each experiment was performed in triplicate.

Apoptotic analysis. Osteoblasts were seeded into 6-well plates ($1x10^5$ cells/well) and cultured in DMEM at 37˚C in 5% CO_2 for 48 h and treated as aforementioned. Cells were harvested with 0.25% trypsin (Sigma-Aldrich; Merck KGaA) at 37˚C in 5% CO_2 for 20 min for apoptotic analysis using the Annexin V apoptosis detection kit (Thermo Fisher Scientific, Inc.) according to the manufacturer's protocol. Cells were stained with Annexin V and PI for 30 min in the dark at room temperature followed by BD FACS Calibur™ flow cytometry analysis using CellQuest Pro 5.1 software (BD Biosciences). Annexin V positive and PI negative stained cells indicated early apoptosis.

Alkaline phosphatase (ALP) staining and enzyme-linked immunosorbent assay (ELISA). Following incubation with ICA (10 μg/l) for 1, 2, 3 and 4 days, calvaria osteoblasts were prepared for ALP staining. A total of $1x10^4$ cells/well were placed into 24-well plates and incubated in the aforementioned conditions until 85% confluence. Cells were subsequently harvested, fixed using 4% paraformaldehyde at 4˚C for 30 min and stained for the analysis of ALP activity with an ALP activity assay kit (BioVision, Inc., Milpitas, CA, USA) according to manufacturer's protocol. Images of stained cells were captured using an Olympus BX51 inverted fluorescent microscope (magnification, x40; Olympus Corporation, Tokyo, Japan). Additionally, the ALP activity of cell cultures was analyzed using an ELISA kit (cat. no. K422; BioVision, Inc.) according to manufacturers' instruction.

Alizarin red staining. For the *in vitro* visualization of nodular patterns and calcium deposition, osteoblasts were stained with Alizarin red S after 21 days of culture in DMEM as previously described (20,21). Briefly, 1,000 cells/well were placed into 24-well plates to reach to 80% confluence. Cells were subsequently harvested, fixed using 4% paraformaldehyde at 4˚C and stained with 2% Alizarin red S (Sigma-Aldrich; Merck KGaA) for 30 min at room temperature. Cells were washed with distilled water prior to observation of plate samples for calcium deposition, which indicates bone nodule formation or osteoblast mineralization, using an Olympus BX51 inverted fluorescent microscope (magnification, x40; Olympus Corporation).

Preparation of proteomics sample. For proteomics analysis, osteoblasts ($1x10^6$ cells/ml) were transferred to a flask and allowed to reach 80% confluence prior to the addition of ICA

(10 μg/l) at 37˚C in 5% CO_2 for 48 h. The secretory proteins from conditioned cell cultures of osteoblasts were prepared for proteomics as previously described (22,23). In brief, the supernatants of the ICA-treated osteoblasts were collected and gathered using TCA-acetone solution (1:3) at -20˚C overnight. Precipitates from centrifugation (750 x g at 4˚C for 5 min) were subsequently washed with acetone, air-dried, quantified using the Bradford assay method (Applygen Technologies, Inc., Beijing, China) (24) and stored at -80˚C.

Two-dimensional electrophoresis (2-DE) and gel image scanning. 2-DE was conducted as described previously (23). Immobilized pH gradient (IPG) strips (17 cm; pH 3-10; GE Healthcare Life Sciences, Uppsala, Sweden) were rehydrated with 150 μg protein for 12-16 h at room temperature, followed by isoelectric focusing (IEF, 60,000 Vh) in a Protean IEF cell (Bio-Rad Laboratories, Inc., Hercules, CA, USA). The IPG strips were subsequently equilibrated as previously described (25) and transferred onto a 12% polyacrylamide gel (Beyotime Institute of Biotechnology, Nanjing, China), which was subjected to the second dimension (200 V, room temperature) in a Protean II XI cell (Bio-Rad Laboratories, Inc.) for 7 h at 6˚C. Polyacrylamide gels were washed and silver stained using a Fast Silver Stain kit according to the manufacturer's protocols (Beyotime Institute of Biotechnology). Finally, the gels were scanned and analyzed using an ImageScanner™ (GE Healthcare Life Sciences) transmission scan with ImageMaster version 5.0 gel image analysis (GE Healthcare Life Sciences). The silver-stained spots with more than 2-fold change in spot intensity and novel spots among groups were considered to be upregulated DEPs. Spots with less than 1-fold change were considered downregulated DEPs. Each experiment was performed in triplicate.

MALDI-TOF/MS. A total of 60 DEP spots were manually cut from gels and digested with trypsin (Gibco; Thermo Fisher Scientific, Inc.) in 96-well plates, according to previously described methods (18). DEP spots were subsequently excised from the polyacrylamide gels. Excised bands were then destained using 50% acetonitrile and 50 mM ammonium bicarbonate at 37˚C for 30 min and digested using trypsin (Gibco; Thermo Fisher Scientific, Inc.) at 37˚C for 16 h. DEPs were subsequently extracted with 50% acetonitrile and 0.1% trifluoroacetic acid 3 times. Gel spot extracts (1.5 μl) were placed into new 96-well plates, vacuum dried and stored at -80˚C prior to MS analysis using a MALDI-TOF/MS system (Bruker Corporation, Ettlingen, Germany) according to instructions as previously described (22,26).

MS database search and alignment of peptide sequences. MS peptide mass fingerprinting (PMF) data was obtained using Mascot Distiller software (v.2.3.2; Matrix Science Ltd., London, UK) (22), and searches of PMF peptide sequences were performed based on the international protein index (IPI) rat FASTA database (v3.31; 41,251 sequences; 21,545,744 residues; ftp://ftp.ebi.ac.uk/pub/databases/IPI). Sequence alignments were generated using the CLC Free Workbench software package (version 4.0.3; Qiagen, Inc., Valencia, CA, USA), and protein properties were identified as previously described (27).

Bioinformatics analysis. In order to investigate the DEP-associated pathways and Gene Ontology (GO) Consortiums, DEP sequences (peptides) were analyzed with the Protein ANalysis THrough Evolutionary Relationships (PANTHER) pathway database (http://www.pantherdb.org/) (28,29). Proteins were classified according to their function and were annotated with ontology terms (PANTHER pathways, GO terms and PANTHER protein class) and sequences are assigned to PANTHER pathways.

Western blot analysis. Western blot analysis was performed to validate expression of several identified potential DEPs. Cellular proteins of calvaria osteoblasts were extracted, quantified as aforementioned. Proteins were subsequently separated by 10% SDS-PAGE (Beyotime Institute of Biotechnology) and electro-transferred onto polyvinylidene difluoride (PVDF) membranes (Invitrogen; Thermo Fisher Scientific, Inc.). Membranes were blocked with 5% milk for 1 h at 4˚C, probed with the primary antibodies against β-actin (cat. no. ab8227; 1:1,000; Abcam, Cambridge, MA, USA), serpin family F member 1 (cat. no. ab14993; PEDF; 1:1,000; Abcam), signal transducing adaptor molecule (cat. no. ab48015; STAM; 1:1,000; Abcam), c-Myc (cat. no. ab32072; 1:1,000: Abcam), protein disulfide isomerase family A, member 3 (cat. no. ab13506; PDIA3; 1:1,000; Abcam), heat shock protein family A member 4 (cat. no. ab2787; HSP70; 1:1,000; Abcam), and nuclear protein, co-activator of histone transcription (cat. no. ab70595; NPAT; 1:1,000; Abcam) overnight at 4˚C. Membranes were subsequently incubated with the appropriate horseradish peroxidase (HRP)-conjugated secondary antibodies (cat. no. ab6721; 1:10,000, Abcam) for 1 h at room temperature. Bands were subsequently visualized using an enhanced chemiluminescence detection reagent (Beyotime Institute of Biotechnology) and were subjected to densitometric analysis with QuantiScan software (v.3.0; BIOSOFT, Cambridge, UK).

Statistical analysis. Experimental data was analyzed using SPSS version 17.0 (SPSS, Inc., Chicago, IL, USA). and is expressed as the mean ± standard deviation. Differences among groups were determined using one-way analysis of variance (ANOVA) followed by Fisher's Least Significant Difference for multiple comparisons. $P<0.05$ was considered to indicate a statistically significant difference.

Results

Identification of osteoblasts. Prior to ICA treatment, isolated calvaria osteoblasts were characterized by ALP and Alizarin red S staining (Fig. 1). At day 3, cells were stained with an ALP assay kit and were observed to have purple stained nuclei accompanied by red-brown stained membrane and cytoplasm (Fig. 1A). Cells were stained with Alizarin red S at day 21 to detect calcium and an irregular red-orange stain was observed, indicating the formation of mineralized bone nodules and the deposition of calcium-rich hydroxyapatite (Fig. 1B).

Effect of ICA on ALP activity and calcium deposition. Osteoblasts were treated with ICA to evaluate the effect of ICA on cell function. Osteoblasts treated with 10 μg/l ICA

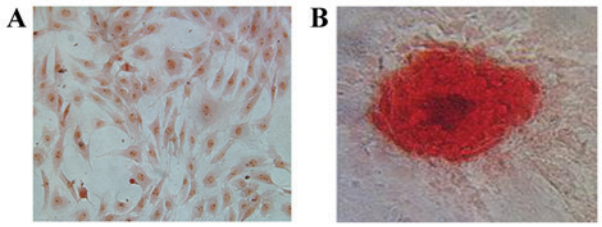

Figure 1. Identification of calvaria osteoblasts. (A) Osteoblasts were stained for Alkaline phosphatase activity 3 days after isolation. (B) Osteoblasts were stained with Alizarin red S following culture for 21 days. All cells were incubated without icariin. Magnification, x40.

for 48 h exhibited the highest ALP activity (P<0.05; Fig. 2A). Cells treated with 10 μg/l ICA demonstrated higher ALP activity compared with cells treated with 20 μg/l ICA at 24, 48 and 72 h time intervals (P<0.05). For Alizarin red S staining analysis, it was confirmed that osteoblasts treated with 10 μg/l ICA had brighter irregular red-orange staining than 20 μg/l ICA-treated cells (Fig. 2B). These results suggested that 10 μg/l ICA concentration was the optimum treatment compared with 20 μg/l for ICA-mediated ALP activation and calcium deposition in osteoblasts.

ICA promotes cell viability and inhibits apoptosis. The MTT assay confirmed that ICA promoted the cell viability of osteoblast in a dose- and time-dependent manner (Fig. 3A). Cells treated with 10 μg/l ICA had significantly increased cell viability at 72 h following ICA incubation (P<0.05). Notably, osteoblasts treated with 20 μg/l ICA had decreased cell viability compared with the 10 μg/l ICA treatment (P<0.05).

Cell cycle distribution analysis revealed that ICA treatment increased the percentage of cells in the S and G2/M phases, and reduced the percentage in the G0/G1 phase (Fig. 3B). As expected, there was also an increase in the percentage of cells in the S and G2/M phase and a decrease in the G0/G1 phase in osteoblasts treated with 10 μg/l ICA compared with those treated with 20 μg/l ICA (P<0.05). Cell apoptosis analysis revealed that ICA inhibited cell apoptosis (Fig. 3C). Osteoblasts treated with 10 μg/l ICA had a significantly lower apoptotic rate when compared with the control and 20 μg/l ICA treated cells (P<0.05). Taken together, it was concluded that ICA increased cell viability and inhibited cell apoptosis. Furthermore, it was determined that the optimum ICA concentration for osteoblast viability was 10 μg/l.

2-DE/MALDI-TOF/MS analysis. Proteomic analysis revealed 60 proteins points that were differentially expressed (with more than two-fold change in spot intensity) or specifically expressed (expression specifically induced by ICA) in osteoblasts treated with 10 μg/l ICA, compared with the control with >750 silver-stained spots (Fig. 4). Bioinformatics analysis identified 56 DEP sequences, which were matched to reference sequences in databases using the CLC Free Workbench software package. Identified DEPS included 22 upregulated DEPs, including STAM binding protein, insulin-like growth factor-binding protein 2 (IGFBP-2) precursor and PEDF. Eight downregulated DEPs were identified, including phosphoglycerate mutase 1 and myosin-1 and succinate dehydrogenase subunit A. A total of 24 specially expressed proteins were identified in ICA-treated osteoblasts, including heat shock proteins [heat shock cognate 71 kDa protein (HSPA8) and heat shock protein, mitochondrial precursor], myc-associated factor X (Max), nuclear protein ataxia-telangiectasia (NPAT) and PDIA3 precursor. Glutaredoxin 5 and translationally controlled tumor protein were DEPs that were lost in ICA treated cells (Table I). A total of four downregulated DEPs in ICA treated osteoblasts were not aligned in the CLC Free Workbench software package.

Bioinformatics analysis. Sequences of these 56 DEPs were subjected to PANTHER pathway database analysis (29,30). DEP enrichment analysis for PANTHER pathways, GO terms (biological processes, molecular function and cellular component) and PANTHER protein classification were performed (Fig. 5). Results revealed that these DEPs were associated with PANTHER pathways, including receptor (PC00197), isomerase (PC00135), calcium-binding protein (PC00060) and signaling molecule (PC00207); enriched into GO terms including 'transporter activity' (GO: 0005215), 'catalytic activity' (GO: 0003824), 'immune system process' (GO: 0002376) and 'cell part' (GO: 0044464); annotated into pathways including Fas (P00020), fibroblast growth factor (FGF; P00021), p53 (P00059) and apoptosis (P04398).

Validation of DEP expression by western blot analysis. Previous reports have demonstrated the association of gene dysregulation with osteoporosis or bone mineral content accumulation, including PEDF (30,31) and PDIA3 (32). Furthermore, NPAT, c-Myc and several other proteins are thought to be involved in the regulation of histone transcription (32,33), calcium metabolism (34) and cell proliferation (35,36). Max associates and interacts with c-Myc, thus forming the c-Myc-Max complex, which has core activating roles in gene expression. Inhibition of c-Myc-Max dimerization formation results in the inhibition of cancer cell proliferation (37,38). HSPA8 is a gene that encodes for an important member of HSP70 protein family (39). Therefore, the expression of HSP70 was investigated. In the present study, Max was identified as a protein that was specifically expressed in response to ICA administration. The expression of c-Myc protein and several identified DEPs in ICA (10 and 20 μg/l) treated osteoblasts was subsequently detected. ICA treatment was demonstrated to upregulate the expression of PEDF, STAM, c-Myc, PDIA3, HSP70 and NPAT. Expression of these DEPs were higher in cells treated with 10 μg/l ICA compared with control cells (P<0.05; Fig. 6). In addition, the expression levels of PEDF, PDIA3, HSP70 and NPAT proteins exhibited by the control cells were not significantly different compared with cells treated with 20 μg/l ICA. These findings were in accordance with the bioinformatics analysis results.

Discussion

The antiosteoporotic activity of ICA has been previously reported (11,12) and was further confirmed in the present study. ICA treatment promoted the viability, ALP activity and calcium deposition of osteoblasts in a dose- and time-dependent manner. Proteomics analysis revealed that the identified proteins were involved in osteogenesis and bone mineral content accumulation via several signaling pathways.

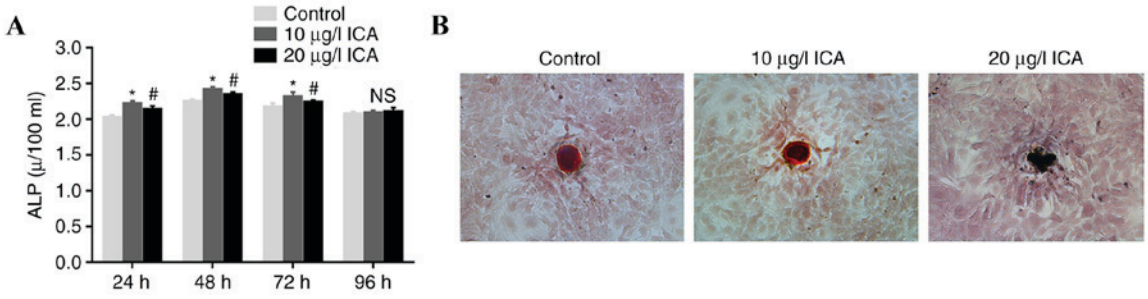

Figure 2. Effect of ICA on ALP activity and calcium deposition. (A) ALP activity was detected using an enzyme-linked immunosorbent assay kit. (B) Calcium deposition in osteoblast cultures was identified by Alizarin red S staining. *P<0.05 vs. control. #P<0.05 vs. 10 μg/l ICA. ICA, icariin; ALP, alkaline phosphatase.

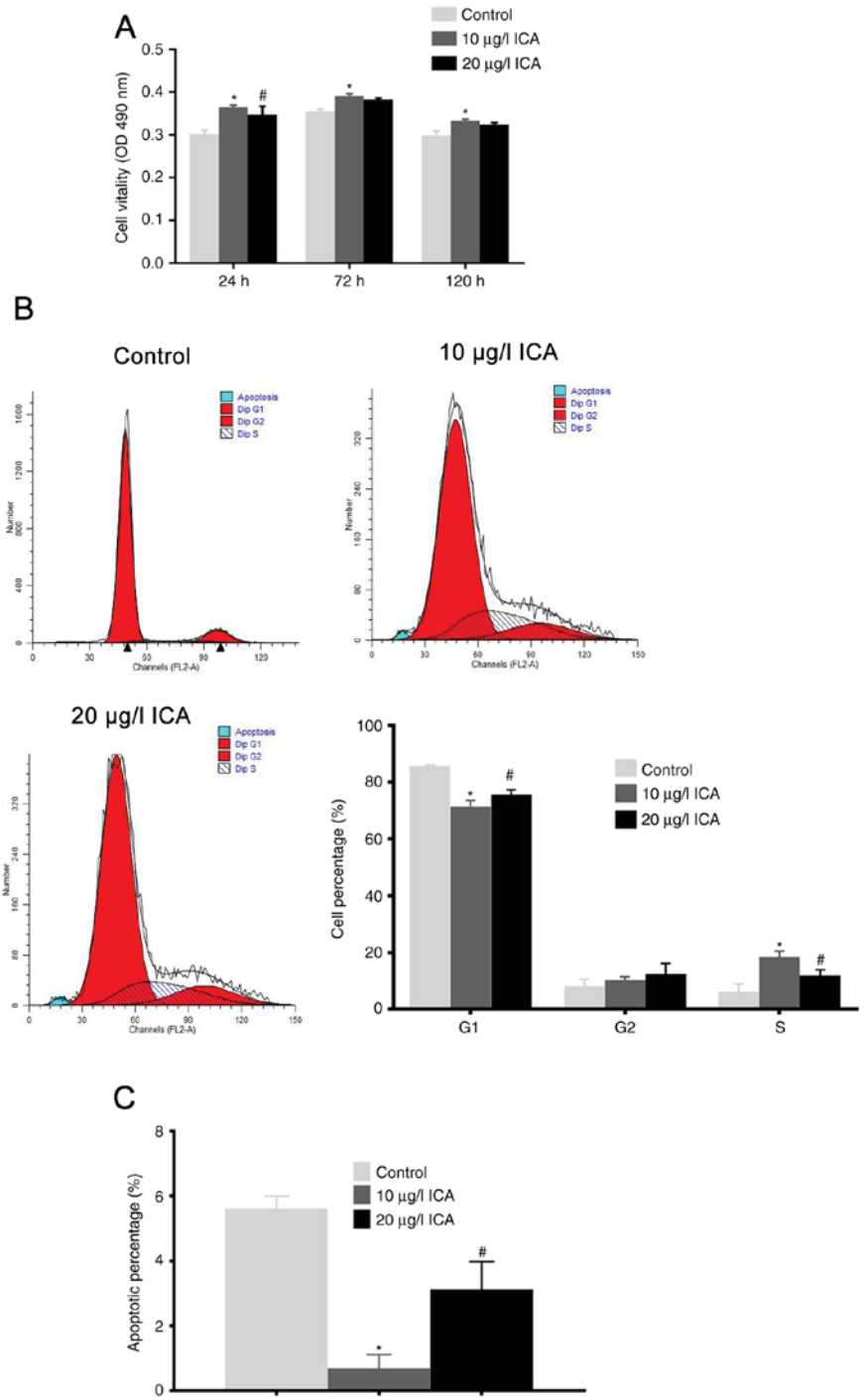

Figure 3. Effect of ICA on cell proliferation and apoptosis. (A) Cell viability was detected with an MTT assay. (B) Cell cycle distribution and (C) cell apoptotic percentage were determined using flow cytometry. *P<0.05 vs. control. #P<0.05 vs. 10 μg/l ICA. ICA, icariin; OD, optical density.

Table I. DEPs in ICA-treated osteoblasts.

A, Upregulated DEPs

Protein point	Sequence number of protein warehouse	Name of protein	Fold-change
59	IPI00231275	Galectin-1	5.7
62	IPI00230937	Phosphatidylethanol-amine-binding protein	5.5
65	IPI00196994	GDP dissociation	6.7
72	IPI00231260	Peroxiredoxin-6	6.8
112	IPI00765011	Follistatin-related protein 1 precursor	7.6
118	IPI00207063	Follistatin-related protein 1 precursor	11.8
123	IPI00464670	Macrophage-capping protein	5.2
127	IPI00778493	Serpinf1 41 kDa protein	9.2
135	IPI00189819	β-actin	8.6
149	IPI00553950	Prolactinregulatory element-binding protein	10.7
155	IPI00200044	STAM binding protein	12.4
186	IPI00370815	T-complex protein 1 subunit theta	11.2
219	IPI00778705	Ephrin type-A receptor 8	7.3
271	IPI00777582	-69 kDa protein	13.0
284	IPI00188921	Collagen alpha-2 (I) chain precursor	17.5
285	IPI00326412	Gamma-enolase	5.7
357	IPI00201060	Lamin-A	5.7
358	IPI00421947	DPPY	5.2
136	IPI00201573	Insulin-like growth factor-binding protein 2 precursor	2.1
159	IPI00209148	Isoform 1 of Heterogeneous nuclear ribonucleoprotein M	3.5
330	IPI00765011	Actin, cytoplasmic 2	4.3
169	IPI00212901	Uncharacterized protein C18 or f19 homolog	5.2

B, Downregulated DEPs

Protein point	Sequence number of protein warehouse	Name of protein	Fold-change
29	IPI00764455	Myosin-1	0.1
101	IPI00421428	Phosphoglycerate mutase 1	0.3
251	IPI00567268	Sdha 72 kDa protein	0.3
105	IPI00362469	6-phosphogluconolactonase	0.7
129	IPI00189819	β-actin	0.6
227	IPI00187662	Cyfip1_predicted 51 kDa protein	0.8
296	IPI00230941	Vimentin	0.6
306	IPI00195929	CAP-Gly domain-containing linker protein 2	0.7

C, DEPs specifically expressed in control

Protein point	Sequence number of protein warehouse	Name of protein	Fold-change
8	IPI00365904	Glutaredoxin 5	-
20	IPI00208306	Translation ally-controlled tumor protein	-
45	IPI00558185	Max (18 kDa protein)	-
91	IPI00213667	Hemiferrin	-
143	IPI00464815	Alpha enolase	-
145	IPI00464815	Alpha enolase	-
147	IPI00464815	Alpha enolase	-
151	IPI00566018	Npat	-

Table I. Continued.

D, DEPs specifically expressed in response to ICA			
Protein point	Sequence number of protein warehouse	Name of protein	Fold-change
153	IPI00767505	γ-actin	-
158	IPI00780207	Dlec1 39 kDa protein	-
174	IPI00212810	Sfrs2 29 kDa protein	-
176	IPI00364170	Spetex-2E	-
180	IPI00192078	Biphenyl hydrolase-like	-
248	IPI00845891	transglutaminase 4	-
263	IPI00208188	Syntaxin-binding protein	-
303	IPI00230941	Vimentin	-
314	IPI00551812	ATP synthase subunit beta, mitochondrial precursor	-
323	IPI00324741	Protein disulfide-isomerase A3 precursor	-
325	IPI00324741	Protein disulfide-isomerase A3 precursor	-
339	IPI00192984	Argbp2 78 kDa protein	-
340	IPI00339148	heat shock protein, mitochondrial precursor	-
342	IPI00208205	Heat shock cognate 71 kDa protein	-
364	IPI00366944	Collagen alpha-1 (III) chain precursor	-
365	IPI00409539	Filamin-A	-
368	IPI00369732	Serine-protein kinase ATM	-
369	IPI00360916	GRIP and coiled-coil domain-containing 2	-

DEP, differentially expressed protein; ICA, icariin.

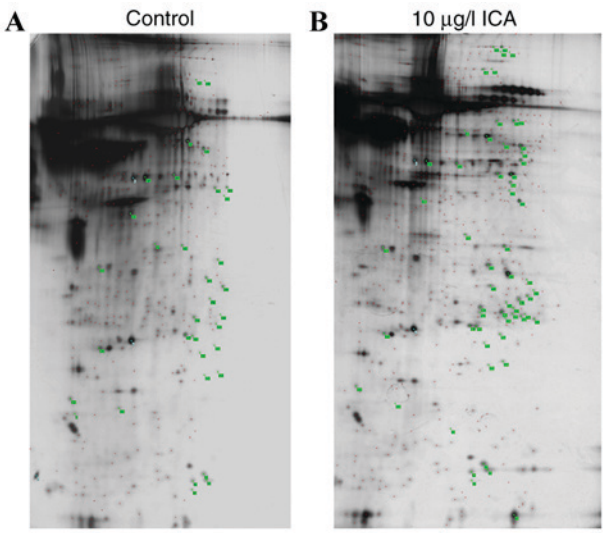

Figure 4. Gel images of obtained from two-dimensional electrophoresis of (A) control osteoblasts and (B) osteoblasts treated with 10 μg ICA. Differentially expressed peptides were marked with green. Protein peptides were marked with red dots. ICA, icariin.

The proliferation inducing effect of ICA was identified in our previous study (40) and other previous research (12,41). ICA is a flavonoid that exhibits anti-apoptosis, cell differentiation and proliferation inducing effects (42,43). In the present study, ICA treatment was demonstrated to promote the proliferation of osteoblasts in a dose-dependent manner. ICA (10 μg/l) demonstrated a more pronounced effect on cell viability, ALP activity and formation of osteoblast mineralized bone nodule, with lower apoptosis percentage compared with 20 μg/l ICA treatment (Figs. 2 and 3). It was confirmed that 10 μg/l ICA was the most effective concentration for osteoblast proliferation and antiosteoporotic activity. This was in accordance with our previous study (40).

Based on the proteomics analysis, 56 proteins were identified as differentially expressed in the 10 μg/l ICA treated osteoblasts compared with the control cells, including PEDF, HSPs, NPAT, PDIA3 and STAM. These proteins were enriched in pathways, GO function terms and PANTHER protein classes including calcium-binding protein, signaling molecule, immune system process and signaling pathways such as Fas, FGF, p53, and apoptosis. As previously reported, p53-B-cell lymphoma 2 (Bcl-2) /Bcl-2 associated protein X-Fas/Fas ligand and FGF-2-p53 are important signaling pathways that modulate apoptosis and proliferation (44,45), demonstrating that the DEPs induced by ICA treatment may be associated with cell differentiation, proliferation and apoptosis. Further validation by western blot analysis revealed that the expression of PEDF, PDIA3, NPAT, NPAT, STAM, HSP70 and c-Myc proteins were upregulated by 10 μg/l ICA administration. This was in accordance with cellular function alterations observed in cells treated with ICA, demonstrating that ICA-induced alterations may be mediated by these proteins.

Previous reports have revealed that the expression of PEDF (30,31), NPAT (32,33) and PDIA3 (32) may directly or indirectly contribute to osteoporosis. PEDF, a 50-kDa secreted

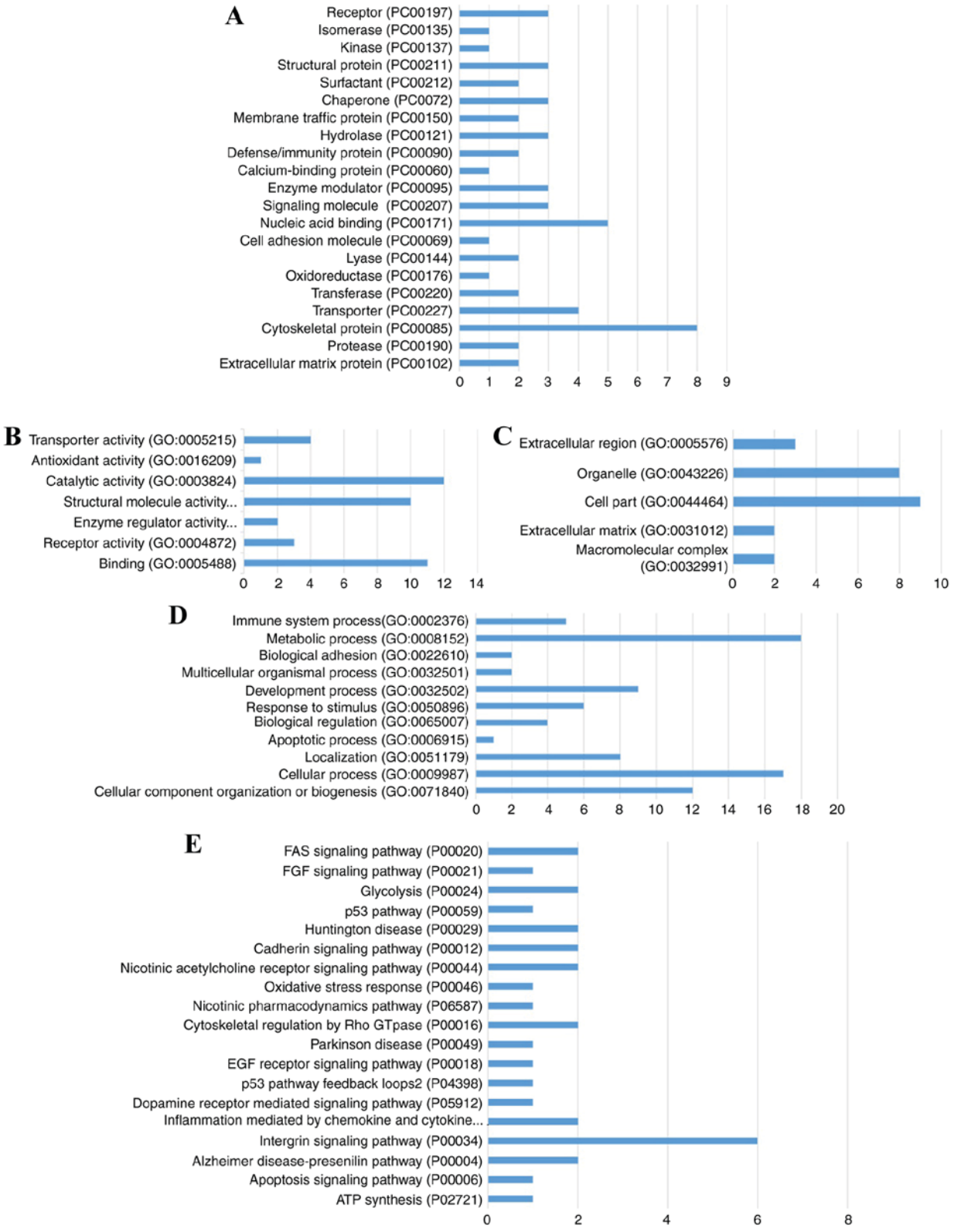

Figure 5. Bioinformatics analysis using pathway database. (A) Identified PANTHER protein classes. GO function terms of (B) molecular function, (C) cellular components and (D) biological process. (E) Terms of PANTHER pathways. Numbers on the x-axis indicate the enriched protein number into corresponding terms.

glycoprotein encoded by SERPINF1, is an endogenous anti-inflammatory factor (46), which also acts as an anti-tumor factor (47,48). PEDF can induce p53- and Fas-mediated cell apoptosis and the expression of anti-inflammatory factors through PPARγ signaling (49). PPARγ is an essential factor for adipocyte differentiation and suppression of its expression has been determined to be crucial for the promotion of osteogenesis and the inhibition of adipogenesis (50,51).

NPAT is an essential factor in histone transcription regulation and acts directly downstream of cyclin E/cyclin-dependent

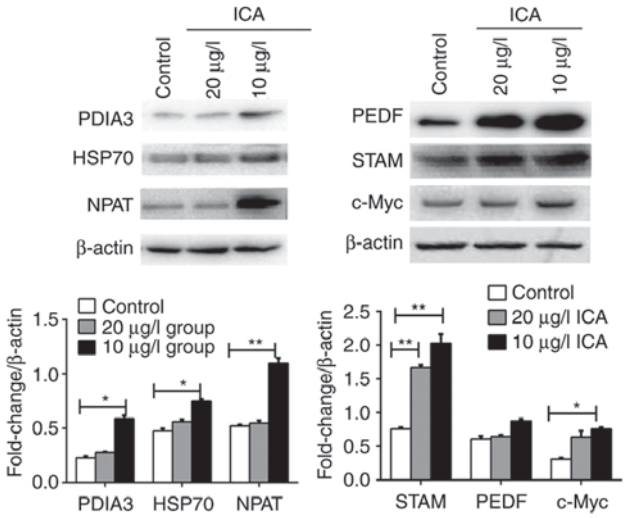

Figure 6. Western blot analysis of the identified differentially expressed proteins in ICA treated osteoblasts. ICA, icariin; PDIA3, protein disulfide isomerase family A, member; HSP70, heat shock protein 70; NPAT, nuclear protein, co-activator of histone transcription; PEDF, serpin family F member 1; STAM, signal transducing adaptor molecule. *P<0.05 and **P<0.01 vs. control.

kinase 2 (52). The phosphorylation or upregulation of NPAT is required for the expression of histone genes, which modulate DNA synthesis and cell cycle proliferation (53). Additionally, NPAT expression correlates with the S phase (53). However, to the best of our knowledge, no reports have investigated the association of PEDF and NPAT with osteoporosis. In the present study, it was confirmed that PEDF and NPAT expression, as well as cell viability in 10 μg/l ICA-treated osteoblasts were upregulated, suggesting that PEDF and NPAT may contribute to osteogenesis via signaling pathways, including Fas and p53 *in vitro*.

Max and c-Myc forms the c-Myc-Max complex, which has a core role in trans-activating gene expression (54,55), whereas the inhibition of c-Myc-Max complex has been previously reported to lead to cell cycle arrest, apoptosis and the inhibition of cancer cell proliferation (37,39). Indo *et al* (56) reported that the inhibition of c-Myc reduces bone-resorbing activity in mature osteoclasts and suppresses the expression of solute carrier family, neutral amino acid transporter (B0), which in turn results in the suppression of osteoclastogenesis. In the present study, it was demonstrated that the expression of Max and c-Myc was significantly upregulated by ICA treatment. Osteoblast apoptosis was inhibited and cell viability and proliferation was enhanced by ICA, suggesting that the formation of the c-Myc-Max complex and subsequent trans-activated gene expression was promoted by ICA treatment.

The PDIA3/phospholipase A2 activating protein receptor complex was reported to be necessary for the Wnt/β-catenin pathway, particularly Wnt5a calcium-dependent pathways in osteoblasts and chondrocytes (32,57). Expression of HSP70 promotes osteoblast differentiation via activation of the mitogen-activated protein kinase signaling pathway (58). Additionally, c-Myc gene products promote HSP70 expression (59) and both c-Myc and HSP70 contribute to cell cycle regulation (60). In the present study, c-Myc, Max, PDIA3 and HSP70 expression was significantly upregulated by ICA treatment. Bioinformatics analysis revealed that these proteins were associated with pathways that may mediate calcium metabolism, suggesting a link between c-Myc, Max, PDIA3 and HSP70 overexpression and osteoporosis, as well as the therapeutic effects of ICA in osteoporosis.

In conclusion, it was demonstrated that ICA treatment promoted proliferation, calcium deposition and inhibited osteoblast apoptosis. Using proteomics analysis, 56 DEPs were identified between cells treated with 10 μg/l ICA and control groups, including PEDF, PDIA3, NPAT, STAM, HSP70 and c-Myc, which may be associated with ICA-mediated osteogenesis differentiation. However, additional experiments should be performed to further elucidate the interaction of these DEPs with ICA-induced osteogenesis and the involvement of these proteins in ICA-induced cell proliferation, calcium accumulation and osteogenesis.

Acknowledgements

Not applicable.

Funding

The present study was funded by the Science Foundation of Traditional Chinese Medicine Administration, Jiangsu Province (grant no. LB09083).

Availability of data and materials

All the data and materials in this manuscript are available from the corresponding author on reasonable request.

Authors' contributions

HY and XZ conceived and designed the experiments. Cell experiments were performed by WQ, YS and YZ. Secretome and data analysis were performed by XZ and NG. Statistical analysis was performed by NY. All authors participated in the writing of the manuscript.

Ethics approval and consent to participate

Animal experimental protocol was approved by the Animal Care Committee of Nanjing University of Chinese Medicine (Nanjing, China). No human subjects were enrolled in this study.

Consent for publication

Not applicable.

Competing interests

The authors declare that there are no competing interests.

References

1. Odén A, McCloskey EV, Kanis JA, Harvey NC and Johansson H: Burden of high fracture probability worldwide: Secular increases 2010-2040. Osteoporos Int 26: 2243-2248, 2015.

2. Zambelli PY Tercier S, Newman CJ and Bregou A: Targeted approach to osteoporosis for children and teenagers. Rev Med Suisse 10: 116-118, 2014 (In French).
3. Tyagi AM, Srivastava K, Mansoori MN, Trivedi R, Chattopadhyay N and Singh D: Estrogen deficiency induces the differentiation of IL-17 secreting Th17 cells: A new candidate in the pathogenesis of osteoporosis. PLoS One 7: e44552, 2012.
4. Kurt-Sirin O, Yilmaz-Aydogan H, Uyar M, Seyhan MF, Isbir T and Can A: Combined effects of collagen type I alpha1 (COL1A1) Sp1 polymorphism and osteoporosis risk factors on bone mineral density in Turkish postmenopausal women. Gene 540: 226-231, 2014.
5. Cheung A, Papaioannou A and Morin S; Osteoporosis Canada Scientific Advisory Council: Postmenopausal osteoporosis. N Engl J Med 374: 2096, 2016.
6. Chen H, Liu N, Xu X, Qu X and Lu E: Smoking, radiotherapy, diabetes and osteoporosis as risk factors for dental implant failure: A meta-analysis. PLoS One 8: e71955, 2013.
7. Miyamoto T: Mechanism underlying post-menopausal osteoporosis: HIF1α is required for osteoclast activation by estrogen deficiency. Keio J Med 64: 44-47, 2015.
8. Ahn HJ, Kim HJ, Kim YS, Kim MS, Huh KH, Kim JH, Lee JH, Jeon KO and Kim SI: Risk factors for changes in bone mineral density and the effect of antiosteoporosis management after renal transplantation. Transplant Proc 38: 2074-2076, 2006.
9. Díez-Pérez A, Adachi JD, Adami S, Anderson FA Jr, Boonen S, Chapurlat R, Compston JE, Cooper C, Gehlbach SH, Greenspan SL, *et al*: Risk factors for treatment failure with antiosteoporosis medication: The global longitudinal study of osteoporosis in women (GLOW). J Bone Miner Res 29: 260-267, 2014.
10. Lee MK, Choi YJ, Sung SH, Shin DI, Kim JW and Kim YC: Antihepatotoxic activity of icariin, a major constituent of Epimedium koreanum. Planta Med 61: 523-526, 1995.
11. Chen KM, Ge BF, Ma HP, Liu XY, Bai MH and Wang Y: Icariin, a flavonoid from the herb Epimedium enhances the osteogenic differentiation of rat primary bone marrow stromal cells. Pharmazie 60: 939-942, 2005.
12. Meng FH, Li YB, Xiong ZL, Jiang ZM and Li FM: Osteoblastic proliferative activity of Epimedium brevicornum Maxim. Phytomedicine 12: 189-193, 2005.
13. Xue L, Wang Y, Jiang Y, Han T, Nie Y, Zhao L, Zhang Q and Qin L: Comparative effects of er-xian decoction, epimedium herbs, and icariin with estrogen on bone and reproductive tissue in ovariectomized rats. Evid Based Complementary Altern Med 2012: 241416, 2012.
14. Yang L, Lu D, Guo J, Meng X, Zhang G and Wang F: Icariin from Epimedium brevicornum Maxim promotes the biosynthesis of estrogen by aromatase (CYP19). J Ethnopharmacol 145: 715-721, 2013.
15. Chen G, Wang C, Wang J, Yin S, Gao H, Xiang LU, Liu H, Xiong Y, Wang P, Zhu X, *et al*: Antiosteoporotic effect of icariin in ovariectomized rats is mediated via the Wnt/β-catenin pathway. Exp Ther Med 12: 279-287, 2016.
16. Liu H, Xiong Y, Zhu X, Gao H, Yin S, Wang J, Chen G, Wang C, Xiang L, Wang P, *et al*: Icariin improves osteoporosis, inhibits the expression of PPARγ, C/EBPα, FABP4 mRNA, N1ICD and jagged1 proteins, and increases Notch2 mRNA in ovariectomized rats. Exp Ther Med 13: 1360-1368, 2017.
17. Li XF, Xu H, Zhao YJ, Tang DZ, Xu GH, Holz J, Wang J, Cheng SD, Shi Q and Wang YJ: Icariin augments bone formation and reverses the phenotypes of osteoprotegerin-deficient mice through the activation of Wnt/β-catenin-BMP signaling. Evid Based Complementary Altern Med 2013: 652317, 2013.
18. Xue L, Jiang Y, Han T, Zhang N, Qin L, Xin H and Zhang Q: Comparative proteomic and metabolomic analysis reveal the anti-osteoporotic molecular mechanism of icariin from Epimedium brevicornu maxim. J Ethnopharmacol 192: 370-381, 2016.
19. Bakker A and Klein-Nulend J: Osteoblast isolation from murine calvariae and long bones. Methods Mol Med 80: 19-28, 2013.
20. Chang H, Jin TY, Jin WF, Gu SZ and Zhou YF: Modulation of isoflavones on bone-nodule formation in rat calvaria osteoblasts in vitro. Biomed Environ Sci 16: 83-89, 2003.
21. Honda H, Tamai N, Naka N, Yoshikawa H and Myoui A: Bone tissue engineering with bone marrow-derived stromal cells integrated with concentrated growth factor in Rattus norvegicus calvaria defect model. J Artif Organs 16: 305-315, 2013.
22. Coutu DL, Wu JH, Monette A, Rivard GE, Blostein MD and Galipeau J: Periostin, a member of a novel family of vitamin K-dependent proteins, is expressed by mesenchymal stromal cells. J Biol Chem 283: 17991-18001, 2008.
23. Zhao Y, Ju F, Zhao Y, Wang L, Sun Z, Liu M and Gao L: The expression of αA- and βB1-crystallin during normal development and regeneration, and proteomic analysis for the regenerating lens in Xenopus laevi. Mol Vis 17: 768-778, 2011.
24. Bradford MM: A rapid and sensitive method for the quantitation of microgram quantities of protein utilizing the principle of protein-dye binding. Anal Biochem 72: 248-254, 1976.
25. Xing X, Lai M, Gartner W, Xu E, Huang Q, Li H and Chen G: Identification of differentially expressed proteins in colorectal cancer by proteomics: Down-regulation of secretagogin. Proteomics 6: 2916-2923, 2006.
26. Ma X, Liu G, Wang S, Chen Z, Lai M, Liu Z and Yang J: Evaluation of sphingolipids changes in brain tissues of rats with pentylenetetrazol-induced kindled seizures using MALDI-TOF-MS. J Chromatogr B Analyt Technol Biomed Life Sci 859: 170-177, 2007.
27. Powell TJ, Strutt T, Reome J, Hollenbaugh JA, Roberts AD, Woodland DL, Swain SL and Dutton RW: Priming with cold-adapted influenza A does not prevent infection but elicits long-lived protection against supralethal challenge with heterosubtypic virus. J Immunol 178: 1030-1038, 2007.
28. Mi H, Muruganujan A, Casagrande JT and Thomas PD: Large-scale gene function analysis with the PANTHER classification system. Nat Protoc 8: 1551-1566, 2013.
29. Mi H and Thomas P: PANTHER pathway: An ontology-based pathway database coupled with data analysis tools. Methods Mol Biol 563: 123-140, 2009.
30. Bogan R, Riddle RC, Li Z, Kumar S, Nandal A, Faugere MC, Boskey A, Crawford SE and Clemens TL: A mouse model for human osteogenesis imperfecta type VI. J Bone Miner Res 28: 1531-1536, 2013.
31. Gattu AK, Swenson ES, Iwakiri Y, Samuel VT, Troiano N, Berry R, Church CD, Rodeheffer MS, Carpenter TO and Chung CH: Determination of mesenchymal stem cell fate by pigment epithelium-derived factor (PEDF) results in increased adiposity and reduced bone mineral content. FASEB J 27: 4384-4394, 2013.
32. Doroudi M: Essential roles of Pdia3/PLAA receptor complex and CaMKII IN $1\alpha,25(OH)_2D_3$ and Wnt5a calcium-dependent signaling pathways in osteoblasts and chondrocytes, 2014.
33. Frank SR, Schroeder M, Fernandez P, Taubert S and Amati B: Binding of c-Myc to chromatin mediates mitogen-induced acetylation of histone H4 and gene activation. Genes Dev 15: 2069-2082, 2001.
34. Kaibuchi K, Tsuda T, Kikuchi A, Tanimoto T, Yamashita T and Takai Y: Possible involvement of protein kinase C and calcium ion in growth factor-induced expression of c-myc oncogene in Swiss 3T3 fibroblasts. J Biol Chem 261: 1187-1192, 1986.
35. Vadde R, Radhakrishnan S, Kurundu HEK, Reddivari L and Vanamala JK: Indian gooseberry (Emblica officinalis Gaertn.) suppresses cell proliferation and induces apoptosis in human colon cancer stem cells independent of p53 status via suppression of c-Myc and cyclin D1. J Funct Foods 25: 267-278, 2016.
36. Zhang W, Shen X, Wan C, Zhao Q, Zhang L, Zhou Q and Deng L: Effects of insulin and insulin-like growth factor 1 on osteoblast proliferation and differentiation: differential signalling via Akt and ERK. Cell Biochem Funct 30: 297-302, 2012.
37. Chen BJ, Wu YL, Tanaka Y and Zhang W: Small molecules targeting c-Myc oncogene: promising anti-cancer therapeutics. Int J Biol Sci 10: 1084-1096, 2014.
38. Zirath H, Frenzel A, Oliynyk G, Segerström L, Westermark UK, Larsson K, Munksgaard Persson M, Hultenby K, Lehtiö J, Einvik C, *et al*: MYC inhibition induces metabolic changes leading to accumulation of lipid droplets in tumor cells. Proc Natl Acad Sci USA 110: 10258-10263, 2013.
39. Banerjee D, Upadhyay RC, Chaudhary UB, Kumar R, Singh S, Ashutosh, G JM, Polley S, Mukherjee A, Das TK and De S: Seasonal variation in expression pattern of genes under HSP70: Seasonal variation in expression pattern of genes underHSP70 family in heat- and cold-adapted goats (Capra hircus). Cell Stress Chaperones 19: 401-408, 2014.
40. Qian W, Yin H and Sun H: Influence of different concentrations of Icariin on osteoblast metabolism of rats. China Med Herald 8: 23-25, 2011 (In Chinese).
41. Song L, Zhao J, Zhang X, Li H and Zhou Y: Icariin induces osteoblast proliferation, differentiation and mineralization through estrogen receptor-mediated ERK and JNK signal activation. Eur J Pharmacol 714: 15-22, 2013.

42. Cao H, Ke Y, Zhang Y, Zhang CJ, Qian W and Zhang GL: Icariin stimulates MC3T3-E1 cell proliferation and differentiation through up-regulation of bone morphogenetic protein-2. Int J Mol Med 29: 435-439, 2012.
43. Zhang DW, Cheng Y, Wang NL, Zhang JC, Yang MS and Yao XS: Effects of total flavonoids and flavonol glycosides from Epimedium koreanum Nakai on the proliferation and differentiation of primary osteoblasts. Phytomedicine 15: 55-61, 2008.
44. Duan P, Hu C, Butler HJ, Quan C, Chen W, Huang W, Tang S, Zhou W, Yuan M, Shi Y, *et al*: 4-Nonylphenol induces disruption of spermatogenesis associated with oxidative stress-related apoptosis by targeting p53-Bcl-2/Bax-Fas/FasL signaling. Environ Toxicol 32: 739-753, 2017.
45. Han Y, Jiang Q, Wang Y, Li W, Geng M, Han Z and Chen X: The anti-proliferative effects of oleanolic acid on A7r5 cells-Role of UCP2 and downstream FGF-2/p53/TSP-1. Cell Biol Int 41: 1296-1306, 2017.
46. Zhang SX, Wang JJ, Gao G, Shao C, Mott R and Ma JX: Pigment epithelium-derived factor (PEDF) is an endogenous antiinflammatory factor. FASEB J 20: 323-325, 2006.
47. Jarvis CL, Nelius T, Martinez-Marin D, Cheerla S and Filleur S: Low-dose cabazitaxel inhibits the growth of prostate cancer cells and enhances the anti-tumor properties of PEDF with greater efficacy than docetaxel. Cancer Res 76: 288, 2016.
48. Nelius T, Hirsch J and Filleur S: PEDF inhibits bone metastases formation, prolongs survival and enhances the antitumor efficacy of low-dose chemotherapy in castration-refractory prostate cancer. Cancer Res 73: 5097, 2013.
49. Ho TC, Chen SL, Yang YC, Liao CL, Cheng HC and Tsao YP: PEDF induces p53-mediated apoptosis through PPAR gamma signaling in human umbilical vein endothelial cells. Cardiovasc Res 76: 213-223, 2007.
50. Sun H, Kim JK, Mortensen R, Mutyaba LP, Hankenson KD and Krebsvach PH: Osteoblast-targeted suppression of PPARγ increases osteogenesis through activation of mTOR signaling. Stem Cells 31: 2183-2192, 2013.
51. Brusotti G, Montanari R, Capelli D, Cattaneo G, Laghezza A, Tortorella P, Loiodice F, Peiretti F, Bonardo B, Paiardini A, *et al*: Betulinic acid is a PPARγ antagonist that improves glucose uptake, promotes osteogenesis and inhibits adipogenesis. Scienti Rep 7: 5777, 2017.
52. Ling Zheng L, Wang FY, Cong XX, Shen Y, Rao XS, Huang DS, Fan W, Yi P, Wang XB, Zheng L, *et al*: Interaction of heat shock protein Cpn10 with the Cyclin E/Cdk2 substrate nuclear protein ataxia-telangiectasia (NPAT) is involved in regulating histone transcription. J Biol Chem 290: 29290-29300, 2015.
53. Zhao J: Coordination of DNA synthesis and histone gene expression during normal cell cycle progression and after DNA damage. Cell Cycle 3: 693-695, 2004.
54. Lin CY, Lovén J, Rahl PB, Paranal RM, Burge CB, Bradner JE, Lee TI and Young RA: Transcriptional amplification in tumor cells with elevated c-Myc. Cell 151: 56-67, 2012.
55. Miller DM, Thomas SD, Islam A, Muench D and Sedoris K: c-Myc and cancer metabolism. Clin Cancer Res 18: 5546-5553, 2012.
56. Indo Y, Takeshita S, Ishii KA, Hoshii T, Aburatani H, Hirao A and Ikeda K: Metabolic regulation of osteoclast differentiation and function. J Bone Miner Res 28: 2392-2399, 2013.
57. Chen J, Olivares-Navarrete R, Wang Y, Herman TR, Boyan BD and Schwartz Z: Protein-disulfide isomerase-associated 3 (Pdia3) mediates the membrane response to 1,25-dihydroxyvitamin D3 in osteoblasts. J Biol Chem 285: 37041-37050, 2010.
58. Chen E, Xue D, Zhang W, Lin F and Pan Z: Extracellular heat shock protein 70 promotes osteogenesis of human mesenchymal stem cells through activation of the ERK signaling pathway. FEBS Lett 589: 4088-4096, 2015.
59. Kingston RE, Baldwin AS Jr and Sharp PA: Regulation of heat shock protein 70 gene expression by c-myc. Nature 312: 280-282, 1984.
60. Taira T, Sawai M, Ikeda M, Tamai K, Iguchi-Ariga SM and Ariga H: Cell cycle-dependent switch of up-and down-regulation of human hsp70 gene expression by interaction between c-Myc and CBF/NF-Y. J Biol Chem 274: 24270-24279, 1999.

This work is licensed under a Creative Commons Attribution-NonCommercial-NoDerivatives 4.0 International (CC BY-NC-ND 4.0) License.